



Methanolysis of PET Waste Using Heterogeneous Catalyst of Bio-waste Origin

Z. T. Laldinpui^{1,2} · Vanlalngaihawma Khiangte^{1,2} · Samson Lalmangaihzuala^{1,2} · Chhakchhuak Lalmuanpuia^{1,2} · Zodinpuia Pachuau² · C. Lalhriatpuia¹ · Khiangte Vanlaldinpuia¹

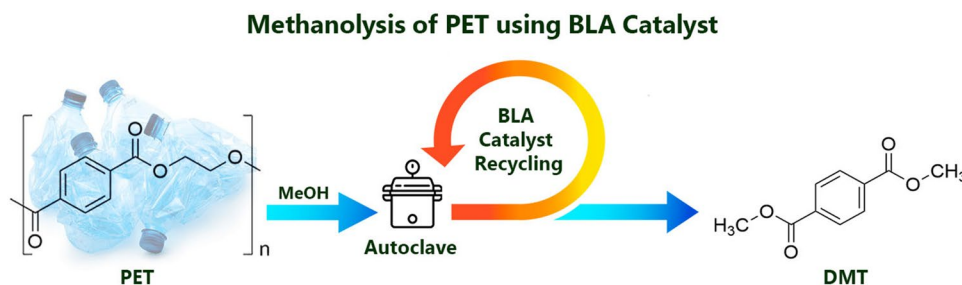
Accepted: 1 October 2021 / Published online: 8 October 2021

© The Author(s), under exclusive licence to Springer Science+Business Media, LLC, part of Springer Nature 2021

Abstract

Decomposition of used poly(ethylene terephthalate) (PET) bottles was accomplished by methanolytic degradation using bamboo leaf ash (BLA) as a green and highly efficient heterogeneous catalytic system. The reaction at 200 °C in an autoclave reactor gave dimethyl terephthalate (DMT) and ethylene glycol (EG) in 78% and 76% yields, respectively. The chemical and physical characteristics of the prepared catalyst were studied using X-ray fluorescence (XRF), Fourier-transform infrared spectroscopy (FTIR), X-ray diffractograms (XRD), Energy dispersive X-ray spectrometry (EDX), Scanning Electron Microscopy (SEM), Transmission Electron Microscopy (TEM), Thermal Gravimetric Analysis (TGA) and Brunauer–Emmett–Teller (BET) analyses. The conversion of PET to DMT and EG was completed within 2 h, and the crude as well as the recrystallized products were characterized using HPLC, NMR and IR. The catalyst, owing to its excellent thermal stability, mesoporous nature, bio-compatibility, cost free, easy preparation, recyclability and efficacy make it an attractive alternative and greener solid catalyst for PET depolymerization.

Graphic Abstract



Keywords Biomass waste · Heterogeneous catalyst · Methanolysis · PET waste · Bamboo leaf ash

Introduction

Plastics have become unescapable in our daily life owing to their low cost of production, durability, high tensile strength and an unabated growth of usage in different sectors. The

annual production of polymeric materials was 381 million tons in 2015 [1], and poly(ethylene terephthalate) (PET) shared 13% of the global plastic output [2, 3]. The thermal and mechanical features are outstanding [4, 5], for which PET is widely used as food and beverage packing materials to the electronics and textile industry [6–8]. The capability to produce a variety of various quality of different molecular weights in a single operation is the primary reason for the extensive application of PET in the pharmaceutical fields [9, 10]. However, extensive use of such polymeric materials, often limited to their single-used coupled with their

✉ Khiangte Vanlaldinpuia
mapuiakhiangte@gmail.com

¹ Department of Chemistry, Mizoram University, Pachhunga University College Campus, Aizawl, Mizoram 796001, India

² Department of Chemistry, Mizoram University, Aizawl, Mizoram 796004, India

non-biodegradability has generated a huge problem with respect to its disposal, with volume and range used increases dramatically in recent years [11, 12]. In addition, when it comes to total solid trash generated globally, PET waste contributes 8 percent and 12 percent by weight and volume of the total garbage produced [13, 14]. It was also estimated that India alone has generated 62 million tons of municipal solid waste every year, which is foreseen to expand at a rate of 1–2% annually, of which plastic wastes account for 5–6% of the total solid waste generated [15, 16]. With these continuous increase in the productions of PET waste and its ability to withstand biological and atmospheric agents, plastic waste has put forward a huge environmental as well as economic problems and there is a high demand for its proper recycling [10, 17–19]. With the exception to its motive towards ecological incentive, recycling of PET waste highly entertained savings of raw petrochemical products and energy [20–23]. Notably, when compared with products obtained from virgin grade resin, the same products obtained from recycled plastic waste results in 50–60% energy saving [3].

Currently, primary recycling, secondary or mechanical recycling, tertiary or chemical recycling, and plastic's energy content retrieval through incineration (quaternary recycling) are the pragmatic accessible recycling processes of PET [24–26]. Primary recycling involves reprocessing of uncontaminated low grade industrial waste generated by the manufacturing industry that is deprived of the desired standard [25]. Mechanical recycling involves segregation of PET materials from its contaminants which are then reutilized by melt extrusion into granules [27]. Chemical recycling, which is referred to as a well adopted and sustainable recycling method transformed PET back to its monomer or secondary value-added products [25, 28, 29]. There have been many reports on chemical recycling methods that use various catalysts. These include aminolysis, ammonolysis, glycolysis, hydrolysis, and methanolysis. [11, 30, 31]. The energy recovery process through incineration of PET waste encounters strong societal opposition due to its high environmental impacts [16, 24]. Only the chemical recycling method, which results in the regeneration of monomers from which polymers are built, was found to meet the criteria of sustainable development among the recycling procedures discussed above [32].

Methanolysis of PET is the breakdown of PET polyesters in the presence of methanol at an elevated temperature ranging from 180 to 280 °C and pressure of 20 to 40 atmosphere, resulting in the production of the desired dimethyl terephthalate monomer and ethylene glycol [33–36]. The main advantages of this method are: i) the quality of the obtained DMT is identical to that of the virgin DMT, ii) the ease of purification of DMT, and iii) easy recovery of EG and methanol. In addition, this method presents a relatively high tolerance to contaminants and hence can treat low quality feedstocks [35,

36]. Different techniques such as liquid methanolysis, vapor methanolysis and supercritical methanolysis were explored [35, 37–40]. As with other depolymerization method, liquid methanolysis in the presence of catalyst proceeds effortlessly. Thus, some divalent metal catalysts including zinc acetate, cobalt acetate, manganese salts, magnesium acetate, calcium phosphate, sodium silicate, lead dioxide, alkali earth metal hydroxides, lead acetate and aluminium triisopropoxide were used as an effective catalyst [24, 25, 35, 40, 41]. Even though the number of research for recycling of PET polyester has increased dramatically, high cost of reaction procedures has become the limiting factor for this method at present [2, 24, 25].

The use of biomass-derived solid catalysts as a substitute to typical heterogeneous catalysts to promote different chemical processes was strongly encouraged in the perspective of environmental and sustainability [42, 43]. As a result, several examples regarding the utilization of carbon-based solid catalysts from biomass waste by various research groups were available recently [42, 44–50]. They are primarily employed as a catalyst in the manufacture of biodiesel and the formation of C–C bonds in organic reactions [42, 51]. Our most recent work has included describing for the first time, a glycolysis technique for old PET that makes use of orange peel ash (OPA) and bamboo leaf ash (BLA) as economically feasible and reusable heterogeneous catalysts [52, 53]. As a result, in addition to our inclination toward the development of more environmentally friendly methods for PET depolymerization [52–54], the present study demonstrated the exploitation of biomass-waste bamboo leaf ash (BLA), which is inexpensive, readily recoverable, and environmentally friendly, as a heterogeneous catalyst for methanolytic conversion of PET to its DMT monomer.

The centerpiece of our research work, “bamboo” is accounted as one among the fast-growing diversity of plants in major parts of the world. The tall, tree-like grasses of the family *Poaceae* were profusely used for a variety of purposes, especially in East and Southeast Asian countries [55]. Mostly, its stems and fibers are a natural resource, widely used in housing construction, home appliances, and handiwork applications [56]. However, the bamboo leaf which has high silica content (30–50%) is considered waste and its applications are almost negligible [57]. Recent studies describe the application of ash obtained from bamboo leaves to cement composites for the generation of pozzolanic materials [58]. Recently, Fatimah and co-workers reported the application of bamboo leaf ash (BLA) supported by ZrO₂ in the microwave-promoted production of biodiesel [56]. Considering the potency, recyclability and renewability, the present communication deals with the application of BLA for depolymerization of poly(ethylene terephthalate) waste bottles through methanolysis, which may perhaps offer an alternative greener route for PET recycling.

Experimental

Materials

Post consumed PET bottles were procured from the market and all the labels along with the caps were removed, washed with distilled water, shredded into 1 mm × 1 mm square chip and dried in an oven. Bamboo (*Melocanna baccifera*) leaves were gathered from Aizawl, Mizoram, India. Methanol, chloroform, commercial ethylene glycol (EG), 2-hydroxyethyl methyl terephthalate (HEMT) and bis-(2-hydroxyethyl) terephthalate (BHET) were purchased from Sigma Aldrich, and no further purification was performed prior to use.

Preparation of BLA Catalyst

The collected bamboo leaf was cleaned thoroughly with distilled water, parched at 80 °C for 8 h and then burnt to ashes. Calcination of the ash was carried out at 700 °C for 4 h, and the greyish color bamboo leaf ash (BLA) was collected, crushed to a fine powder, sieved and then stored in a sample vial at room temperature.

Characterization of PET Waste

The thermal analysis of the post consumed PET was carried out using PerkinElmer DSC 6000 under an inert atmosphere with nitrogen flow of 20 ml min⁻¹. PET samples (2–4 mg) were then heated from 50 to 300 °C at a rate of 20 °C min⁻¹ using indium (In) as a standard for measuring enthalpy of fusion (ΔH_f). Degree of Crystallinity of PET was calculated from the enthalpy change obtained from DSC analysis by taking 140 J g⁻¹ as ΔH_f of pure crystalline PET using the following equation [59]:

$$\text{Crystallinity\%} = \frac{\text{Enthalpy of fusion}}{140 \text{ J/g}} \times 100. \quad (1)$$

Characterization of the Catalyst

To analyze the morphological structure, crystallinity, chemical content of the prepared BLA catalysts FTIR, XRF, XRD, TEM, SEM, EDX, BET and TGA analyses were performed. FT-IR spectra of the prepared catalyst was obtained using KBr disks on Spectrum BX FT-IR, Perkin Elmer (ν_{max} in cm⁻¹). SEM images and determination of the elemental composition was performed on JSM-6360, Jeol and ESEM EDAX XL-30, respectively. TEM images were obtained using JEM-2100, 200 kV instrument. X-ray fluorescence (XRF) of the catalysts were screened through PANalytical, Axios mAX. For the investigation of crystalline properties

of the catalyst, Powder X-ray diffraction (XRD) patterns were obtained from Philips, Xpert MPD. The N₂ adsorption–desorption isotherm of the prepared BLA was documented using Quanta chrome Nova-1000 surface area and porosity analyzer. The thermogravimetric analysis (TGA) was recorded on Perkin Elmer TGA 4000 and the thermal stability of the catalyst was analyzed at a temperature ranging from 30 to 999 °C.

Methanolysis of PET Waste

PET depolymerization was conducted using Shilpent Teflon Lined Hydrothermal Autoclave (50 mL) charged with 480 mg of PET flakes (2.50 mmol), 100 mg of BLA catalyst and 5 mL of methanol. The autoclave was then plunged to an oil bath at 200 °C temperature. As soon as the autoclave was immersed, the temperature of the oil bath dropped significantly and it was then gradually heated to the predetermined temperature within 20 min. When the fixed temperature had been reached, the reaction was kept constant for 2 h. After the reaction had ended, the BLA catalyst was isolated by way of filtration and then washed with 40 ml of heated MeOH. The filtrate was enabled to cool down to room temperature and then placed in a refrigerator at 2 °C for 4 h, where a crystallized DMT separates out, which was filtered, dried and weighed (78%). The filtrate was distilled under reduced pressure to recover methanol and ethylene glycol. The white crystalline residue was collected and analyzed using HPLC and NMR. The percentage conversion and yield recrystallized DMT were calculated using the equations given below:

$$\begin{aligned} \text{Conversion of PET (\%)} &= \frac{\text{weight of initial PET} - \text{weight of recovered PET}}{\text{weight of initial PET}} \quad (2) \\ &\times 100. \end{aligned}$$

$$\text{Yield of DMT monomer (\%)} = \frac{\text{Actual yield of DMT monomer}}{\text{Theoretical yield of DMT}} \times 100. \quad (3)$$

Product Characterization

Nuclear Magnetic Resonance Spectroscopy (¹H NMR and ¹³CNMR) were recorded on Bruker, 400 MHz Avance III spectrometer in DMSO-d₆. FT-IR spectra were recorded on a Spectrum BX FT-IR, Perkin Elmer in the range of 4000–500 cm⁻¹. HPLC (High Pressure Liquid chromatography) was recorded on Waters 1525 binary pump and Waters UV detector 2489 using Spherisorb ODS2 5 μm, 4.6 × 250 mm analytical column at 254 nm. The solution of methanol and water at 70/30 volume fraction at a flow

rate of 1 mL/minute was used as a mobile phase. The UV–Vis spectra were recorded on Labtronics UV–Vis Spectrophotometers Model-LT-2202, and the samples were dissolved in chloroform (5 mg/mL).

Results and Discussion

Post-consumer PET Characterization

Physical properties of PET such as glass transition temperature, heat of fusion and melting temperature were studied and is highlighted in Table 1. From the analysis, the glass transition temperature T_g of post consumed PET was found to be in between that of amorphous and crystalline [60], with clear PET having the highest T_g of 79 °C, followed by light yellow color PET with 78 °C T_g , while green color PET has the lowest T_g with 75 °C. Moreover, enthalpy of fusion (ΔH_f) of post consumed PET was determined by heating it to a temperature well above its melting point (300 °C), and cooling it to a lower temperature (50 °C), which is then again reheated to 300 °C temperature using Indium as a standard reference for calibration. It was observed that green color PET has the highest ΔH_f with 60.0128 J g⁻¹, while clear and light-yellow color PET have 55.1033 J g⁻¹ and 54.5185 J g⁻¹ respectively. As aforementioned, enthalpy of fusion (ΔH_f) obtained was employed for calculating the degree of crystallinity, which is a measure of the orderliness of the polymer chain for each sample. As a result, green color PET having the highest enthalpy of fusion has the highest degree of crystallinity with 42.86%, next to clear PET with 39.35 crystallinity %, while light yellow color has the lowest crystalline component with 38.94%. In general, the rate of decomposition of PET material was known to be inversely related to their degree of crystallinity, i.e., rate of degradation becomes sluggish with an increase in degree of crystallinity [61]. However, crystallinity studies of different colored PET bottles showed that the percentage crystallinity are almost the same, thus, explaining

Table 1 Thermal properties of poly(ethylene terephthalate) samples obtained from DSC analysis

Sample	Weight of sample (in mg)	T_{mo} (°C) ^a	T_m (°C) ^a	ΔH_f (J g ⁻¹) ^a	T_g (°C) ^a	Crystallinity (%) ^b
Clear PET	3.200	239.11	255.38	55.1033	79	39.35
Green color PET	2.600	237.63	253.81	60.0128	75	42.86
Light-yellow color PET	2.000	236.05	254.24	54.5185	78	38.94

^aMelt onset temperature (T_{mo}), melt end temperature (T_m), enthalpy (ΔH_f) and glass transition temperature (T_g) measured at a heating rate of 20 °C min⁻¹ by DSC

^bDegree of crystallinity was determined based upon 140 Jg⁻¹ for the ΔH_f of 100% crystalline PET

Table 2 XRF analysis of BLA catalyst

Sl. No	Chemical formula	Concentration (%)
1	SiO ₂	76.02
2	SO ₃	6.892
3	CaO	4.783
4	K ₂ O	2.876
5	Fe ₂ O ₃	2.341
6	MnO	1.888
7	MgO	1.277
8	P ₂ O ₅	0.64
9	Al ₂ O ₃	0.529
10	Na ₂ O	0.134
11	Cr ₂ O ₃	0.124
12	TiO ₂	0.117
13	CuO	0.114
14	ZnO	0.092
15	SrO	0.053

a uniform depolymerization time for each colored PET bottle.

Catalyst Characterization

XRF analysis was performed to evaluate the compositions of the prepared catalyst and the findings are shown in Table 2. The composition was found to be of 76.026% silicon dioxide (SiO₂), 6.892% sulphur trioxide (SO₃), 4.783% calcium oxide (CaO), 2.876% potassium oxide (K₂O), 2.341% ferric oxide (Fe₂O₃), 1.888% manganese oxide (MnO) and 1.277% magnesium oxide (MgO) as the major constituent. Apart from these, oxides of phosphorus, aluminium, sodium, chromium, titanium, etc., were found to be present in minor quantities for the catalytic activation.

X-ray Photoelectron Spectroscopy (XPS) evaluation was performed out to decode the elemental configuration of the fresh BLA catalyst (Fig. 1). After extensive study of the wide-scan spectrum, the availability of Si, O, C, Ca, and K as the major elements in the external region can be

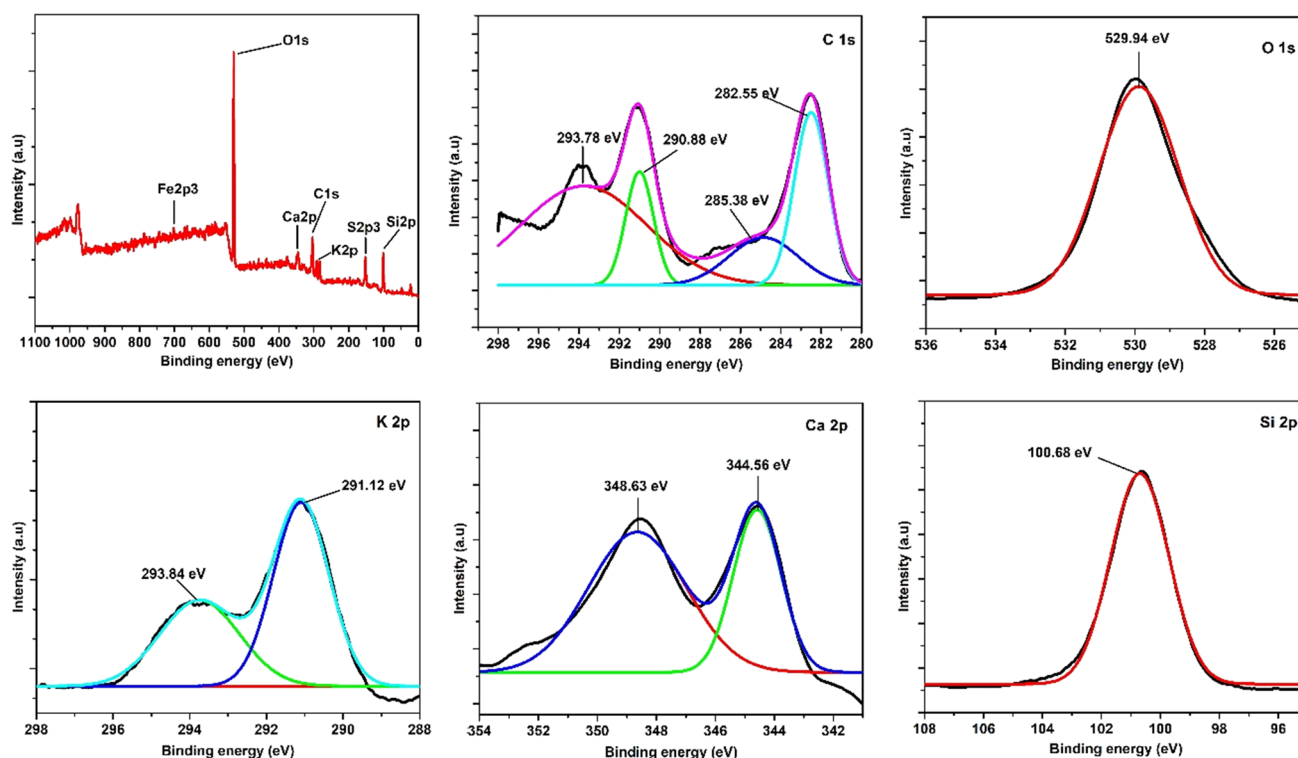


Fig. 1 XPS analysis of BLA catalyst

confirmed. On deconvolution, the C1s spectra comprise four distinct peaks. The peaks at 285.38 and 293.78 eV may be assigned to the presence of C–C and C=O of metal carbonates on the ash particle. The deconvoluted O1s spectra shows one hump, positioned at binding energy of 529.94 eV, which may be attributed to the presence of metal oxides. Moreover, on deconvolution, the K2p spectra present two peaks at 293.84 and 291.12 binding energies, which was assigned to K_2O and K_2CO_3 . Likewise, the Ca2p spectra also shows two peaks at 348.63 and 344.56 eV, which confirms the presence of $CaCO_3$ and CaO respectively. Furthermore, a single peak located at binding energy of 100.68 eV within the Si2p spectra credited the presence of an abundant SiO_2 compound of the catalyst.

The presence of crystalline complex in BLA was identified by XRD analysis wherein compounds in the form of their carbonates and oxides were determined (Fig. 2a). It can be seen that strong characteristic diffraction peaks observed at $2\theta = 20.817^\circ$, 26.566° , 50.088° , 29.405° , 45.688° corresponding to (100), (011), (003), (104), and (221) planes confirm the presence of SiO_2 and $CaCO_3$ (JCPDS reference file No: 89–1961, 89–8936, 89–8945, 86–2334, 87–1863). Typical spectra of the catalyst profusely demonstrate silica as the dominant phase, and other diffraction peaks at 47.422° , 54.755° , and 59.822° correlated to (113), (141), and (060) planes (JCPDS reference no: 86–0294, 86–0305, 73–1539)

were due to the presence of Na_2CO_3 and MnO_2 . Beside these, the occurrence of Fe_2O_3 , SO_3 , K_2O , K_2CO_3 , CaO, and MgO were observed at 35.750° , 36.840° , 39.422° , 40.222° , 42.355° , and 43.089° which corresponds to (110), (112), (220), (221), (422), and (200) planes, matching well with the existing library JCPDS reference no: 89-8104, 73-2169, 47-1701, 70-0292, 02-1088, 87-0653, 88-0107, respectively. In continuation, the results of XRF and XRD data were strongly supported by EDX analysis showing O (48.01%), Si (32.27%), Ca (8.98%), K (4.61%) as the primary constituent elements with Mg (1.59%), Mn (1.25%), Al (1.12%), P (0.83%), S (0.49%), and Cl (0.32%) as the less abundant elements in the ash sample (see Supporting Information Fig. S11).

Functional group analysis (FTIR) of the catalyst was performed as shown in Fig. 2b. The peaks at 1082 cm^{-1} and 796 cm^{-1} highlights the asymmetric stretching and bending vibrations of Si–O bond. The peak at 3442 cm^{-1} is associated with water molecule absorbed by the catalyst. The appearance of peaks at 1641 and 1446 cm^{-1} can be attributed to the C–O vibrations of metal carbonates in the catalyst, respectively.

Brunauer–Emmett–Teller (BET) method was used to evaluate the surface area of the catalyst, and Barrett–Joyner–Halenda (BJH) model was employed to detect the average pore size distribution. These methods elaborate the surface

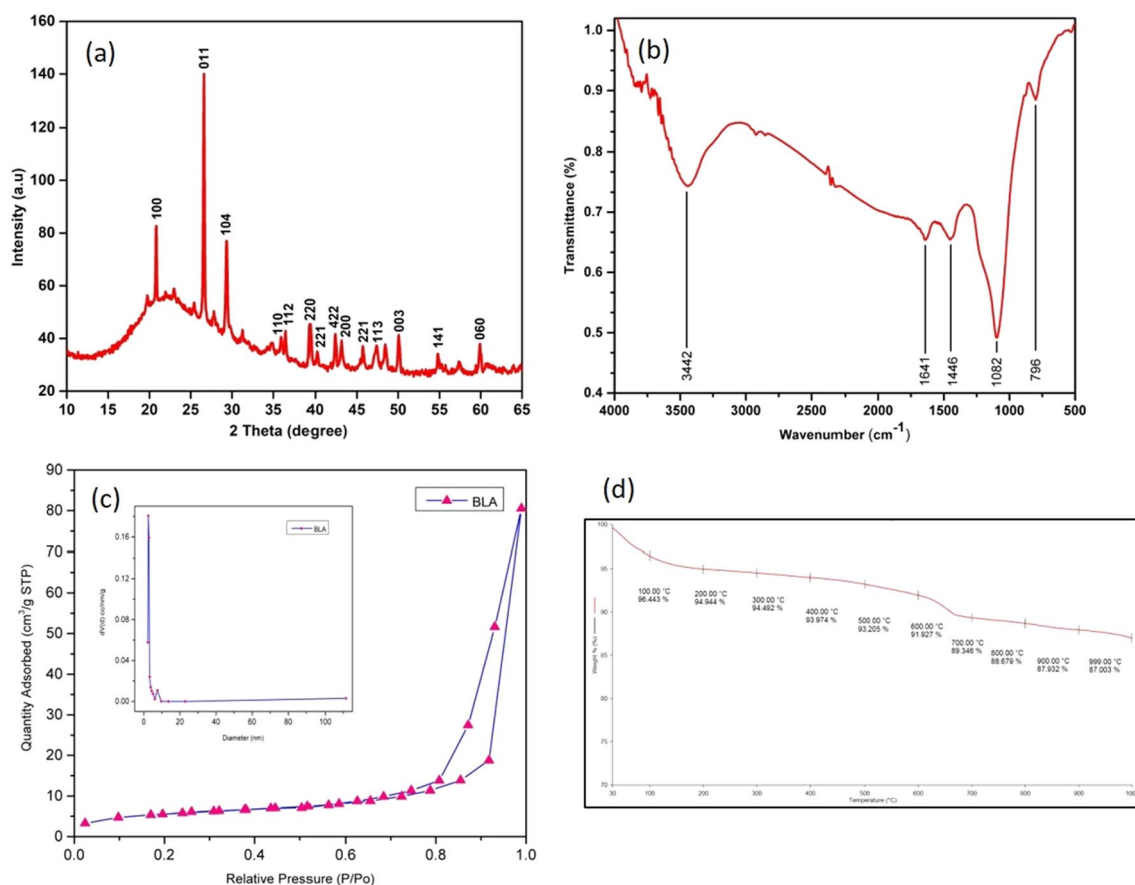


Fig. 2 Bamboo leaf ash **a** XRD pattern, **b** FT-IR spectra, **c** nitrogen adsorption–desorption isotherm (inset: BJH pore size distribution), and **d** TGA thermogram

area and pore size of the ash catalyst, determining the total specific area in m^2/g unit at standard temperature and pressure, thereby providing an important information regarding the effects of external porosity of the catalyst. The surface area, pore diameter and pore volume of the catalyst were found to be $21.847 \text{ m}^2/\text{g}$, 136.84 \AA , and $0.127 \text{ cm}^3/\text{g}$, respectively. The N_2 adsorption–desorption isotherm (Fig. 2c) showed a typical type-IV isotherm, which is the characteristics of mesoporous materials [62]. The higher BET external area and mesoporous characteristics of the material may contribute to the higher catalytic activity of the ash catalysts towards transesterification reaction.

Thermal Gravimetric Analysis (TGA) of the prepared BLA was presented to investigate its thermal inertness with temperature (Fig. 2d). Results showed that 5% of the initial weight was lost between 30 and 200 $^\circ\text{C}$, corresponding to the removal of water content from the catalyst. Moreover, additional dropping in the weight of the ash material typically corresponds to oxygenation of carbon moiety of the ash material [63].

SEM and TEM images delineated the external outline of the ash samples. The SEM images (Fig. 3a, b) illustrates

that the outline of bamboo leaf ash particles is rough and spongy with an agglomerated assembly of microporous and mesoporous structures. Besides, TEM images (Fig. 3c, d) also show aggregated irregular globular surface of the catalyst with different size distributions, having an average spherical diameter ranging from 10 to 50 nm approximately (Fig. 4).

Analysis of Solid Products

It was reported earlier that methanolytic decomposition of PET results in DMT production as the main component with the generation of several byproducts such as 2-Hydroxyethylmethyl terephthalate (HEMT), bis-(2-hydroxyethyl) terephthalate (BHET), BHET dimer, DMT dimer and oligomers in small amount [40]. In our case, analysis of the final crude product by HPLC revealed the presence of EG, BHET, HEMT and DMT at a retention time of 2.177, 3.259, 4.273 and 7.354, respectively. This was confirmed by evaluation of HPLC studies of commercially available EG, BHET, HEMT and recrystallized DMT monomer (see Supporting Information Figs. S1–S5).

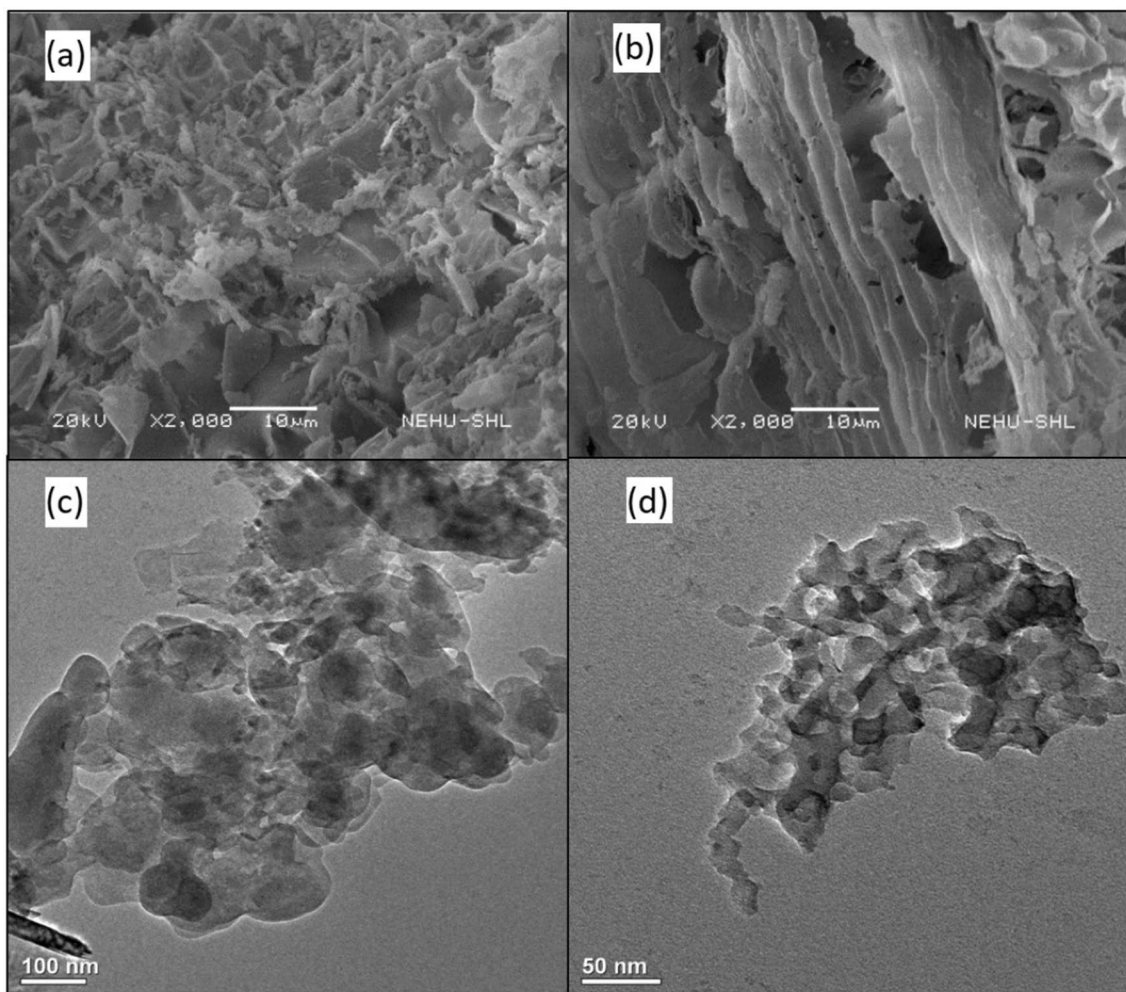


Fig. 3 SEM images (a, b) and TEM images (c) and d of BLA

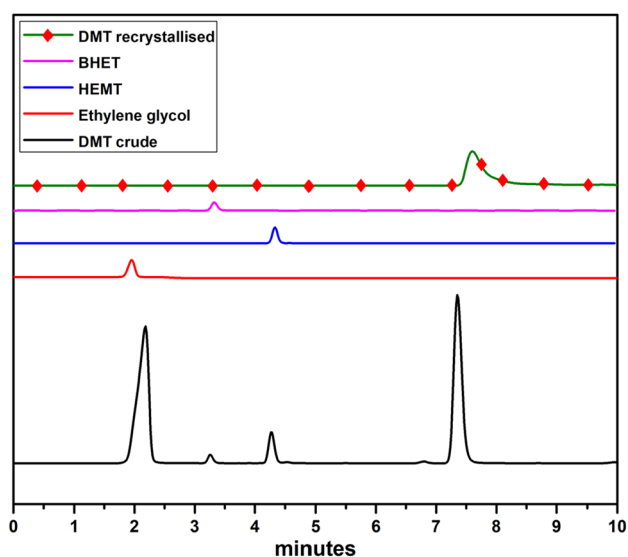
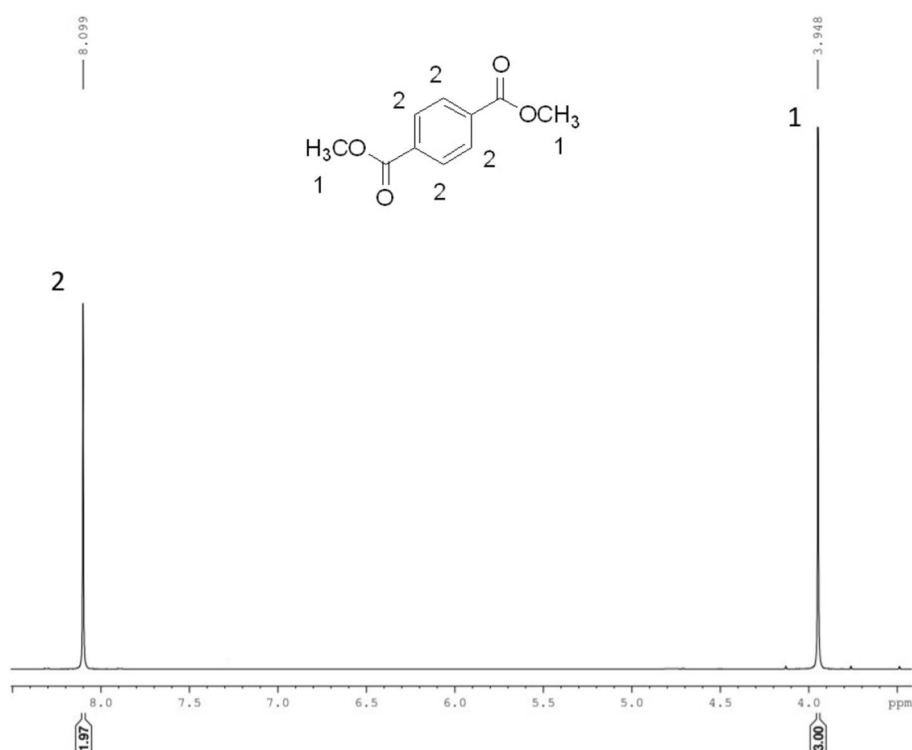


Fig. 4 HPLC data of recrystallized DMT, commercial BHET, commercial HEMT, commercial EG and the crude product

Purification of the crude reactions was then performed based on the method highlighted in the experimental section to obtain pure DMT monomer, and it was characterized by using NMR and IR spectroscopy. In its ^1H NMR spectra, singlets at $\delta = 3.948$ ($-\text{OCH}_3$) and 8.099 ($\text{Ar}-\text{H}$) ppm (Fig. 5) confirm the formation of the desired product which was further substantiated by the resonances at $\delta = 166.85$, 134.48 , 130.13 and 53.01 ppm in its ^{13}C NMR spectra (see Supporting Information Fig. S7). The FT-IR spectra of recrystallized DMT shows an absorption band at 1703 cm^{-1} , indicating the existence of esters functionality (see Supporting Information Fig. S8). The strong absorption bands observed at 1262 and 1087 cm^{-1} may be allocated to the stretching vibrations of methyl and C–O bond, correspondingly. Existence of the methyl group was confirmed by the vibrational band at 2952 cm^{-1} .

Fig. 5 ^1H NMR spectra of recrystallized DMT



Proposed Reaction Pathway for Methanolysis of PET Waste

The framework of the possible reaction mechanism for methanolysis of PET BLA as a catalyst is given in Fig. 6. It is generally accepted that for any reaction involving exchange of ester functionality, the solid-based catalyst should exhibit several basic sites, high surface area as well as large pore diameter to provide an effective transition from start to finish [64–66]. In this commentary, based on the data available from characterization of the catalyst and experimental results, we consider that the occurrence of several elements like Ca, K, Fe, Mg etc., available in order of their oxides and carbonates have introduced an effective strategy for the degradation of PET waste granules. Earlier studies have also reported that decomposition of PET waste through transesterification reaction was subjected to Lewis acid–base synergistic effect [67]. Hence, for each successful conversion, a nucleophilic methoxide ion was generated with the abstraction of a proton from -OH group of methanol by the anionic sites (such as O^{2-} , CO_3^{2-}) present within the catalyst. Subsequently, the methoxide ion interacts with the cationic sites (Mn^{2+} , K^{2+} , Ca^{2+} , Mg^{2+} etc.) of the catalyst, which initially assembled nucleophilic attack on electron deficient carbonyl of esters group to form a tetrahedral intermediate. As the reaction proceeds further, a rearrangement reaction takes place where the esters bond gets cleaved, and the polymeric substrates experienced a new C–O bond formation between

the carbonyl carbon of PET polyester and oxygen from methanol. As a result, the PET chain cleaved, decreasing the chain length to form oligomers and finally into a dimethyl terephthalate (DMT) monomer as the major product. Besides DMT, coupling of the acyl $-\text{OCH}_2\text{CH}_2-$ group with proton adsorbed by the catalyst results in the formation of ethylene glycol in the reaction mixture.

Effect of Reaction Parameters on Depolymerization of PET Waste

The impact of catalyst loading on PET to DMT conversion at 200 °C with 5 ml of methanol is summarized in Fig. 7a. We experienced that the degree of polymerization and DMT yield increases exponentially with every rise in BLA loading. As such, when PET degradation reaction was carried out with the exclusion of our catalyst, even after 48 h of time, only 71% PET transformation and 0.8% DMT yield were obtained. The maximum yield of DMT monomer was obtained using 100 mg of the catalyst, furnishing 73% yield within 2 h of reaction time. However, we also observed that a further increase in the catalysts loading above 100 mg does not result in any significant enhancement of the yield. HPLC analysis of the crude product with 120 mg of BLA loading indicates an escalated formation of BHET, HEMT and other byproducts which otherwise could not be isolated under normal recrystallization procedure (see Supporting Information Fig. S13). Hence, we envisage that after reaching the optimal catalyst concentration, the depolymerization

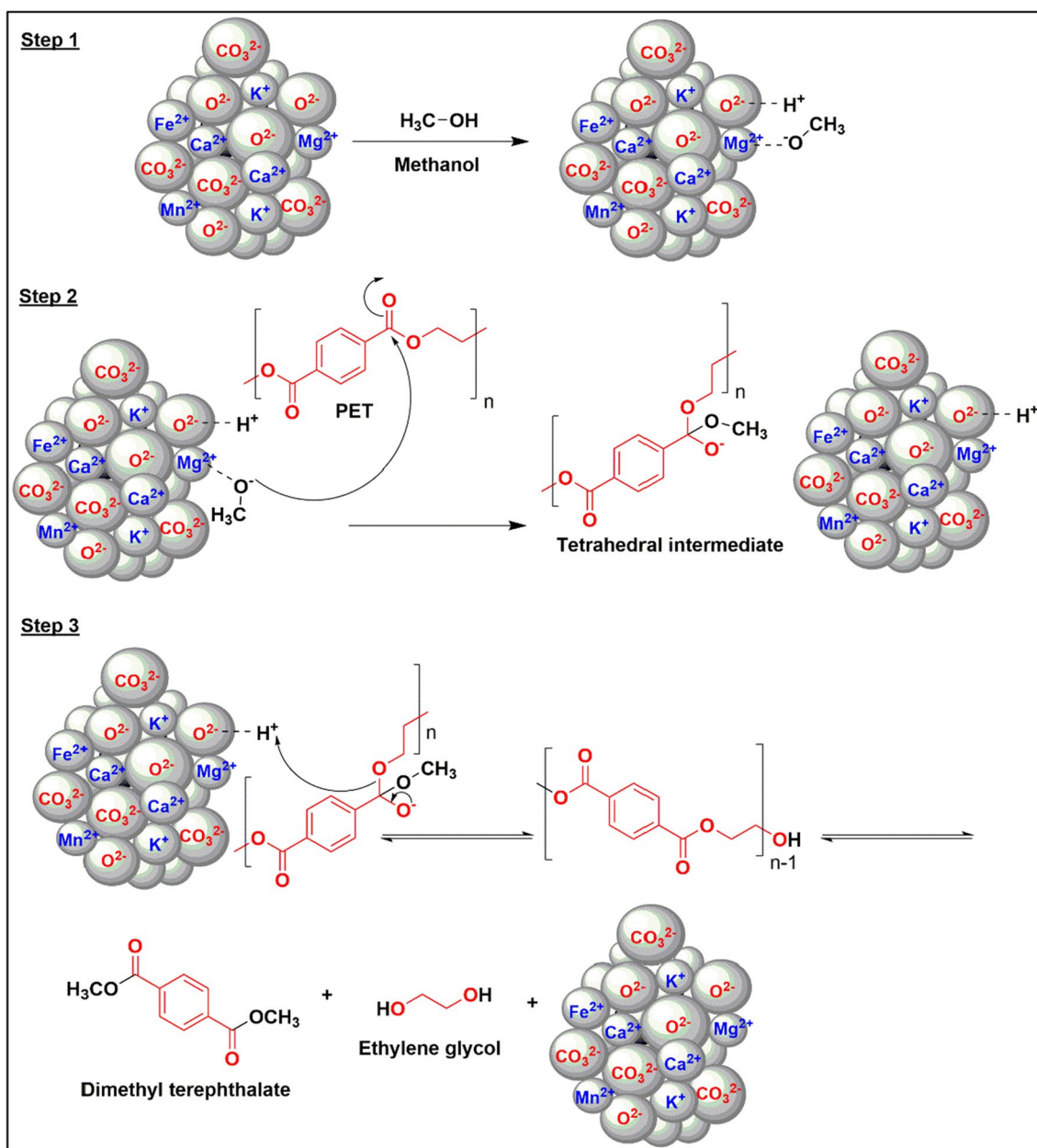


Fig. 6 Plausible reaction pathway for methanolysis of PET using BLA

occurs hastily to form DMT, which is then repolymerized to form oligomers and other byproducts, thereby creating a chemical equilibrium [41].

Reactions were performed to analyze the influence of time of reaction and temperature of reaction on the breakdown of PET waste to its monomeric DMT units. At a varying reaction time ranging from 1 to 4 h, depolymerization of 2.50 mmol of PET waste was set up while keeping the catalyst loading and methanol concentration constant at 20 wt% and 5 ml, respectively. The level of PET decomposition and the formation of DMT monomer escalated sharply when the reaction period was increased from 1 to 2 h (Fig. 7b). But

beyond that, there is a slight decrease in the overall yield of DMT which may be due to an increase in the formation of other depolymerized products as shown by HPLC analysis (see Supporting information Fig. S14). The initial increase and then subsequent decrease in the DMT formation can be explained on the grounds of their equilibration process. Generally, degradation of PET by methanolysis is believed to start from the chip surface and occurs at random places in the polymeric chain, producing the oligomers, and finally, generating DMT and EG [41]. As the reaction advanced with time, the monomer was then repolymerized to form

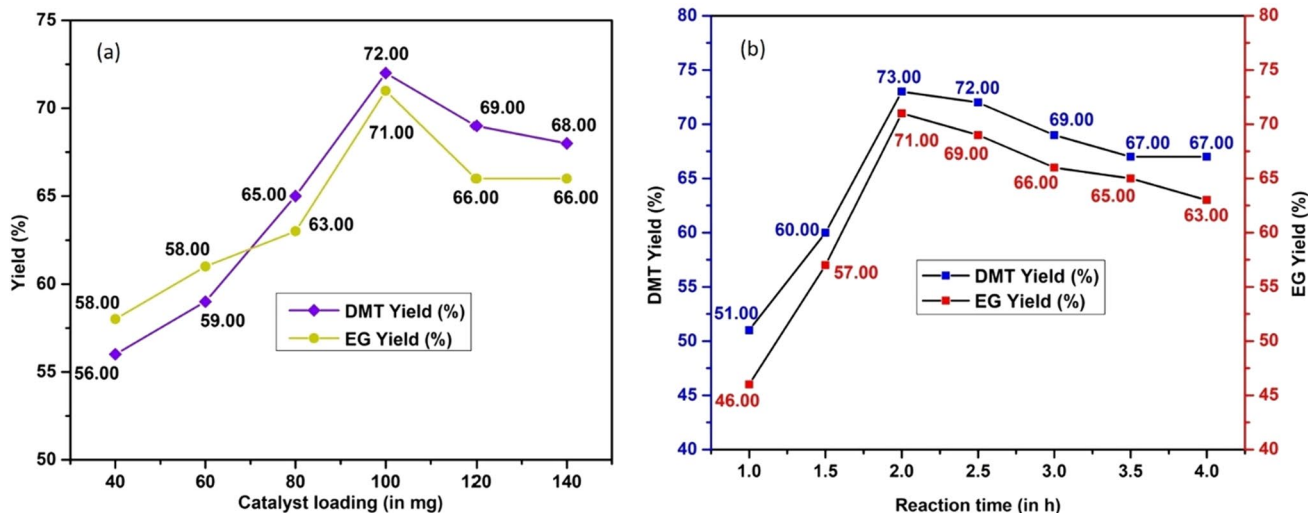


Fig. 7 a Influence of catalyst charging on methanolysis of PET. Reactions were carried out with 480 mg of PET, 5 mL of methanol and varied amount of catalyst at 200 °C for 2 h. b Influence of time on

DMT yield. Reaction condition of 200 °C, 480 mg of PET, 100 mg of BLA and 5 mL of methanol

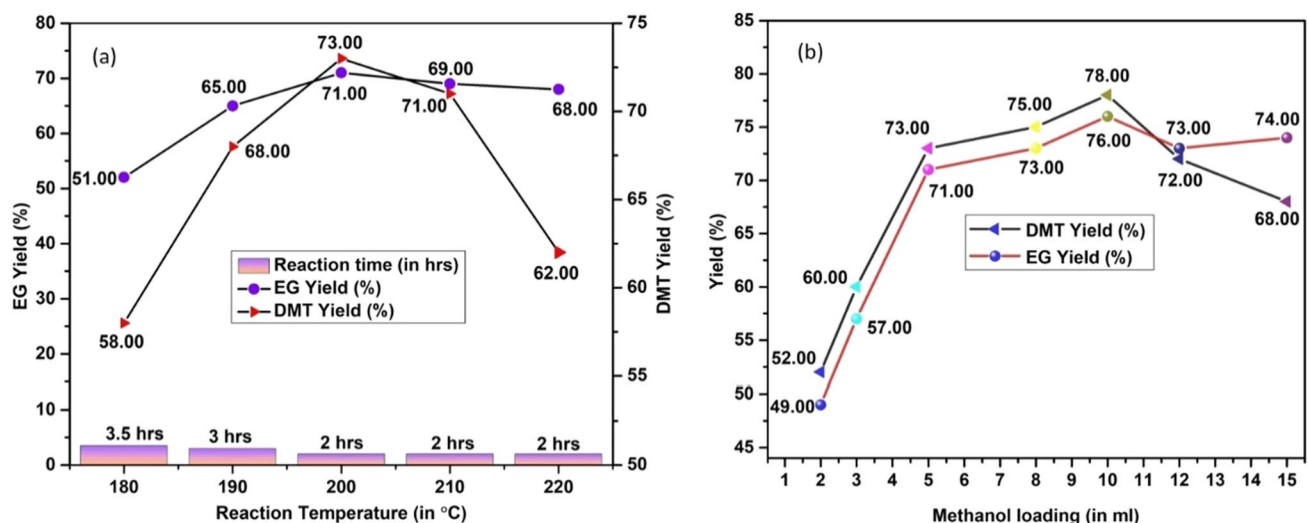


Fig. 8 a Influence of temperature on methanolysis of PET. Reactions with 480 mg of PET, 100 mg of BLA, 5 mL of methanol at 200 °C. b Influence of methanol concentration on methanolysis of PET. Reac-

tions with 480 mg of PET, 100 mg of BLA and varied amounts of methanol concentration for 2 h at 200 °C

the dimers and/or oligomers, thus reducing the overall DMT yield.

We also observed that a 180 °C reaction condition did not seem to attain completion even after a prolonged reaction time of about 4 h. It was seen that rising of the reaction temperature greatly influenced the rate of depolymerization as shown in Fig. 8a. The best result was obtained at 200 °C, where complete degradation with the highest DMT yield was achieved within 2 h of reaction time. A sharp decrease in DMT yield was seen at 220 °C with an increase in oligomers production.

The impact of methanol concentration on the degradation of post-consumer PET was also investigated and is charted in Fig. 8b. The result indicates that the rate of PET degradation and the DMT obtained upsurge rapidly with every rise in methanol loading from 2 to 10 mL. But after reaching its optimal concentration of 10 mL of MeOH, the DMT yield decreases even with a further rise in methanol concentration, and an augmented formation of the oligomers and other byproducts were again detected in the HPLC data. This indicates that an optimal methanol concentration is required for

the whole effectiveness of the protocol when other reaction parameters are kept constant.

Methanolysis of Color PET Bottles

Under the optimized condition, methanolysis of green, light-yellow and red PET bottles were also investigated (see Supporting information Table S6). The reactions were completed within 2 h giving good selectivity for DMT monomer. Most of the color observed separates out during recrystallization process, and any persisting pigments can be deleted by adding activated charcoal upon recrystallization [28, 52]. The samples were dissolved in chloroform (5 mg/ml) and the absorbance of DMT obtained from colored as well as clear bottle was recorded on UV–Vis spectrophotometer at 350–800 nm wavelength range (Fig. 9a).

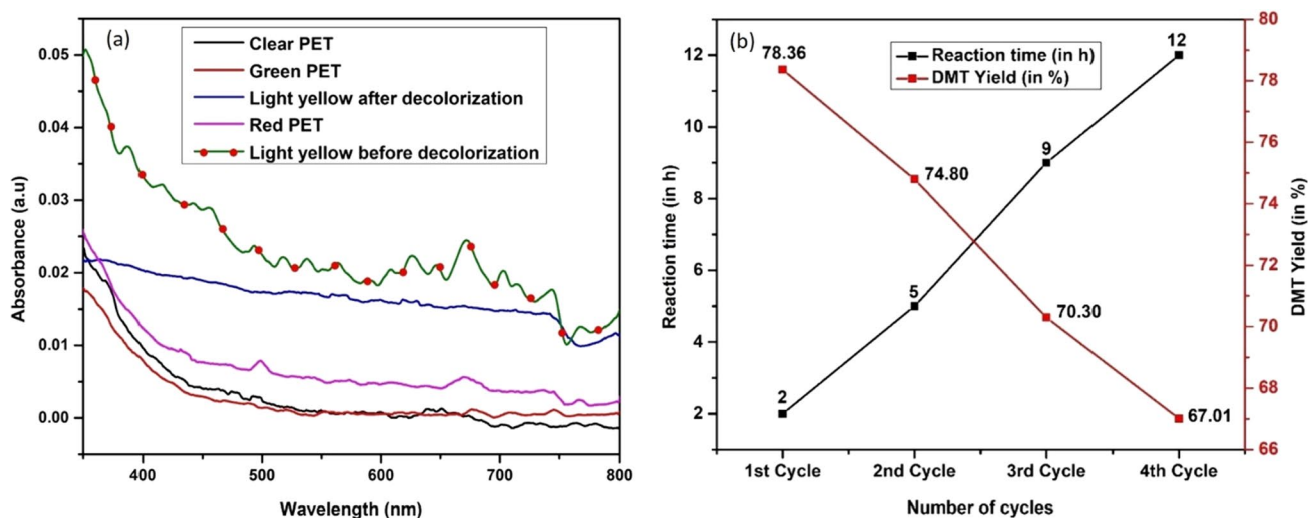


Fig. 9 **a** UV–vis spectra of DMT monomer derived from clear, green, light-yellow (before and after decolorization) and red PET bottles. **b** Reusability of BLA on degradation of PET. Reaction condition: 480 mg PET, 100 mg BLA, 10 mL methanol, 200 °C

Table 3 Comparison of the efficacy of the prepared catalyst with some reported procedure

Sl.no	Catalyst	Catalyst (in wt%)	Temperature (in °C)	Pressure (in atm)	Time	MeOH (mol. eq.)	Yield (in %)	References
1	–	–	300	–	30 min	71.27	55	[39]
2	–	–	310	99.4	30 min	83.98	98	[68]
3	–	–	270	108.562	40 min	28.5	96	[40]
4	[Al(O ⁱ Pr) ₃]	10	200	–	2 h	95.00	67.30	[41]
5	KOH	69	100	–	30 min	16.78	96	[69]
6	Zn (OAc) ₂	1	180	–	55 min	9.5	–	[24]
7	K ₂ CO ₃	14.35	25	–	24 h	50.00	93.50	[67]
8	BLA	20	200	–	2 h	98.87	78	This work

Table 4 Rate constant (k), correlation coefficient (R^2), activation energy (E_a) and pre-exponential factor (A) of various kinetic models

Order of reaction	Rate constant at various temperature (K)				R^2	E_a (kJ/mol)	A (s^{-1})
	453	463	473	483			
1 st	4.32×10^{-5}	3.57×10^{-5}	4.37×10^{-5}	4.75×10^{-5}	0.582	132.48	Nd
Pseudo 1st	6.88×10^{-5}	10.55×10^{-5}	18.18×10^{-5}	17.19×10^{-5}	0.875	59.943	604.861
2 nd	2.44×10^{-5}	1.96×10^{-5}	2.36×10^{-5}	2.55×10^{-5}	0.115	nd	nd

For the recovered catalyst, SEM and TEM images reveal the retention of agglomerated structure with microporous and mesoporous nature identical to the virgin catalyst. EDX studies of the fresh and recovered BLA catalyst disclose a substantial loss of Fe, Mg, Mn, K, and Ca concentration in the recovered catalyst, while Si remains almost the same. These remarkable changes in the concentration may affect the percentage yield of the depolymerization product with the recovered catalyst.

Several methodologies have been employed for methanolysis of PET, and are listed in Table 3. The demand of high temperature, long reaction time, tedious purification process, presence of co-solvent for better achievements as well as high catalyst loading are some of the major disadvantages of the prior reported procedures. In order to control and conquer these problems, experimental design was demonstrated to reduce the overall cost of PET recycling using inexpensive, eco-friendly and waste origin biomass derived BLA as a heterogeneous catalyst. The ease of catalyst separation and recovery, ease of preparation and handling, excellent reusable property and high selectivity towards DMT formation are some of the advantages of the prepared BLA catalyst.

Kinetic Studies of PET Methanolysis

Random scission and specific scission are said to be involved in the degradation of PET, with the former being the more common type [38]. Random scission occurs at the beginning of the process, while specific scission occurs at the end of the process. Meanwhile, it was discovered that the initial stage of the process takes a longer time than expected and is assumed to be the step that determines the rate of the reaction. Table 4 contains the results of the calculated different kinetic parameters for various kinetic models as proposed by Basumatary et al. [70], based on the experimental findings.

These data were used to generate Arrhenius plots of $\ln k$ against the reciprocal of absolute temperature ($1/T$), which are depicted in Figs. S15, S16, and S17 (see Supporting information Figs. S15–S17). When the plots are fitted with a linear function and the graphical interpretation and evaluation are performed, the correlation coefficient (R^2) values for first order, pseudo first order, and second order kinetics are 0.582, 0.875, and 0.115, respectively, for the three types of kinetics. Figure S16 recommended that the reaction occur in this

order owing to its greatest R^2 value. Additionally, the activation energy (E_a) of the BLA catalyzed PET Methanolysis was determined to be 59.943 kJ/mol as compared to 95.31 kJ/mol [71], 66.5 kJ/mol [67] and 56 kJ/mol [72] for some reported literatures.

Conclusion

In conclusion, unknown to prior technique, we have investigated and described methanolysis of PET waste bottles using BLA as a transesterification catalyst to regenerate the DMT monomer in excellent yield. The catalyst being a waste origin, hence free, was actively used for rapid and complete decomposition of PET. Its easy preparation and handling, environmentally friendliness and high efficacy are some notable advantages of this solid catalyst. The degree of conversion and selectivity for the desired monomer was greatly influenced by the methanol concentration, catalyst loading, reaction temperature and time period. Despite the presence of ample amount of SiO_2 (~ 76%) in the catalyst, the availability of other basic sites (such as CaO, K_2O etc.) was observed to promote the depolymerization reaction. Thus, with its high efficacy and heterogeneous active surface, the BLA is found to be an efficient, environmentally benign catalyst to offer a greener protocol to chemically treat post-consumer PET bottles.

Supplementary Information The online version of this article contains supplementary material available <https://doi.org/10.1007/s10924-021-02305-0>.

Acknowledgements This work was supported by Science and Engineering Research Board, New Delhi, India, File no EEQ/2017/000505. ZT Laldinpui and Samson Lalmangaihuuala gratefully acknowledge CSIR and UGC for financial support through Junior Research Fellowship. The authors thank SICART, SAIF-NEHU, BIT-Bangalore and IIT Roorkee for sample analyses.

Author's Contribution ZTL: formal analysis, investigation, writing—review and editing. VK: formal analysis, investigation, writing—reviewing and editing. SL: software, data curation, writing—original draft preparation. CL: visualization, software, writing—reviewing and editing. ZP: supervision, writing—reviewing and editing. C. Lalmhriatpua: supervision, validation, writing—reviewing and editing. KV: conceptualization, methodology, validation, resources, project administration, supervision, funding acquisition, writing—reviewing and editing.

Declarations

Conflict of interest The authors report no declarations of interest.

References

- Ritchie H, Roser M (2018) Plastic pollution. Our World in Data. References—Scientific Research Publishing. <https://scirp.org/reference/referencespapers.aspx?referenceid=3053948>. Accessed 25 Sept 2021
- Jehanno C, Pérez-Madrilal MM, Demarteau J et al (2019) Organocatalysis for depolymerisation. *Polym Chem* 10:172–186. <https://doi.org/10.1039/C8PY01284A>
- Karayannidis GP, Achilias DS (2007) Chemical recycling of poly(ethylene terephthalate). *Macromol Mater Eng* 292:128–146. <https://doi.org/10.1002/mame.200600341>
- López-Fonseca R, Duque-Ingunza I, de Rivas B et al (2010) Chemical recycling of post-consumer PET wastes by glycolysis in the presence of metal salts. *Polym Degrad Stab* 95:1022–1028. <https://doi.org/10.1016/j.polydegradstab.2010.03.007>
- López-Fonseca R, Duque-Ingunza I, de Rivas B et al (2011) Kinetics of catalytic glycolysis of PET wastes with sodium carbonate. *Chem Eng J* 168:312–320. <https://doi.org/10.1016/j.cej.2011.01.031>
- Welle F (2011) Twenty years of PET bottle to bottle recycling—an overview. *Resour Conserv Recycl* 55:865–875. <https://doi.org/10.1016/j.resconrec.2011.04.009>
- Padhan RK, Sreeram A (2019) Chemical depolymerization of PET bottles via combined chemolysis methods. *Recycl Polyethyl Terephthalate Bottles*. <https://doi.org/10.1016/B978-0-12-811361-5.00007-9>
- Awaja F, Pavel D (2005) Recycling of PET. *Eur Polym J* 41:1453–1477. <https://doi.org/10.1016/J.EURPOLYMJ.2005.02.005>
- Nadkarni VM, Rath AK (2002) Blends of thermoplastic polyesters: sections 1–5. *Handb Thermoplast Polyesters*. <https://doi.org/10.1002/3527601961.CH19A>
- Malik N, Kumar P, Shrivastava S, Ghosh SB (2017) An overview on PET waste recycling for application in packaging. *Int J Plast Technol* 21:1–24. <https://doi.org/10.1007/s12588-016-9164-1>
- Sinha V, Patel MR, Patel JV (2008) Pet waste management by chemical recycling: a review. *J Polym Environ* 18(18):8–25. <https://doi.org/10.1007/S10924-008-0106-7>
- Geyer B, Lorenz G, Kandelbauer A (2016) Recycling of poly(ethylene terephthalate)—a review focusing on chemical methods. *Express Polym Lett* 10:559–586. <https://doi.org/10.3144/expresspolymlett.2016.53>
- Leng Z, Padhan RK, Sreeram A (2018) Production of a sustainable paving material through chemical recycling of waste PET into crumb rubber modified asphalt. *J Clean Prod* 180:682–688. <https://doi.org/10.1016/j.jclepro.2018.01.171>
- Atta AM, El-Kafrawy AF, Aly MH, Abdel-Azim A-AA (2007) New epoxy resins based on recycled poly(ethylene terephthalate) as organic coatings. *Prog Org Coat* 58:13–22. <https://doi.org/10.1016/j.porgcoat.2006.11.001>
- Managing Plastic Waste in India: An agenda for action. <https://www.cseindia.org/managing-plastic-waste-in-india-an-agenda-for-action-10361>. Accessed 25 Sept 2021
- Tshifularo CA, Patnaik A (2020) Recycling of plastics into textile raw materials and products. *Sustain Technol Fash Text*. <https://doi.org/10.1016/B978-0-08-102867-4.00013-X>
- Khoonkari M, Haghghi AH, Sefidbakht Y et al (2015) Chemical recycling of PET wastes with different catalysts. *Int J Polym Sci*. <https://doi.org/10.1155/2015/124524>
- Al-Sabagh AM, Yehia FZ, Eshaq G et al (2016) Greener routes for recycling of polyethylene terephthalate. *Egypt J Pet* 25:53–64. <https://doi.org/10.1016/J.EJPE.2015.03.001>
- Dutt K, Soni RK (2013) A review on synthesis of value added products from polyethylene terephthalate (PET) waste. *Polym Sci Ser B* 55(55):430–452. <https://doi.org/10.1134/S156090413070075>
- Neale CW, Hilyard NC, Barber P (1983) Observations on the economics of recycling industrial scrap plastic in new products. *Conserv Recycl* 6:91–105. [https://doi.org/10.1016/0361-3658\(83\)90034-6](https://doi.org/10.1016/0361-3658(83)90034-6)
- Throne JL (1987) Effect of recycle on properties and profits: algorithms. *Adv Polym Technol* 7:347–360. <https://doi.org/10.1002/adv.1987.060070401>
- Yoda N (1999) Corporate management in the age of global environmental awareness: a case study of PET-bottle-recycling issues in Japan. *Polym Int* 48:944–951. [https://doi.org/10.1002/\(sici\)1097-0126\(199910\)48:10%3c944::aid-pi252%3e3.0.co;2-y](https://doi.org/10.1002/(sici)1097-0126(199910)48:10%3c944::aid-pi252%3e3.0.co;2-y)
- Farahat MS, Abdel-Azim A-AA, Abdel-Raowf ME (2000) Modified unsaturated polyester resins synthesized from poly(ethylene terephthalate) waste, 1. Synthesis and curing characteristics. *Macromol Mater Eng* 283:1–6. [https://doi.org/10.1002/1439-2054\(20001101\)283:1%3c1::AID-MAME1%3e3.3.CO;2-M](https://doi.org/10.1002/1439-2054(20001101)283:1%3c1::AID-MAME1%3e3.3.CO;2-M)
- Siddiqui MN, Redhwi HH, Achilias DS (2012) Recycling of poly(ethylene terephthalate) waste through methanolic pyrolysis in a microwave reactor. *J Anal Appl Pyrolysis* 98:214–220. <https://doi.org/10.1016/j.jaap.2012.09.007>
- Raheem AB, Noor ZZ, Hassan A et al (2019) Current developments in chemical recycling of post-consumer polyethylene terephthalate wastes for new materials production: a review. *J Clean Prod* 225:1052–1064. <https://doi.org/10.1016/J.JCLEPRO.2019.04.019>
- Damayanti, Wu H-S (2021) Strategic possibility routes of recycled PET. *Polymers* 13:1475. <https://doi.org/10.3390/POLYM13091475>
- Shamsaei M, Aghayan I, Kazemi KA (2017) Experimental investigation of using cross-linked polyethylene waste as aggregate in roller compacted concrete pavement. *J Clean Prod* 165:290–297. <https://doi.org/10.1016/j.jclepro.2017.07.109>
- Fukushima K, Coulembier O, Lecuyer JM et al (2011) Organocatalytic depolymerization of poly(ethylene terephthalate). *J Polym Sci Part A* 49:1273–1281. <https://doi.org/10.1002/pola.24551>
- Lorenzetti C, Manaresi P, Berti C, Barbiroli G (2006) Chemical recovery of useful chemicals from polyester (PET) waste for resource conservation: a survey of state of the art. *J Polym Environ* 14:89–101. <https://doi.org/10.1007/s10924-005-8711-1>
- López-Fonseca R, González-Marcos MP, González-Velasco JR, Gutiérrez-Ortiz JI (2009) A kinetic study of the depolymerisation of poly(ethylene terephthalate) by phase transfer catalysed alkaline hydrolysis. *J Chem Technol Biotechnol* 84:92–99. <https://doi.org/10.1002/jctb.2011>
- Paszun D, Spychaj T (1997) Chemical recycling of poly(ethylene terephthalate). *Ind Eng Chem Res* 36:1373–1383. <https://doi.org/10.1021/IE960563C>
- Achilias DS, Karayannidis GP (2004) The Chemical recycling of PET in the framework of sustainable development. *Water Air Soil Pollut Focus* 4:385–396. <https://doi.org/10.1023/B:WAFO.0000044812.47185.0f>
- Kang MJ, Yu HJ, Jegal J et al (2020) Depolymerization of PET into terephthalic acid in neutral media catalyzed by the ZSM-5

- acidic catalyst. *Chem Eng J* 398:125655. <https://doi.org/10.1016/j.cej.2020.125655>
34. Bartolome L, Imran M, Lee KG et al (2014) Superparamagnetic γ -Fe₂O₃ nanoparticles as an easily recoverable catalyst for the chemical recycling of PET. *Green Chem* 16:279–286. <https://doi.org/10.1039/C3GC41834K>
 35. Han M (2019) Depolymerization of PET bottle via methanolysis and hydrolysis. *Recycl Polyethyl Terephthalate Bottles*. <https://doi.org/10.1016/B978-0-12-811361-5.00005-5>
 36. Polyethylene Terephthalate Waste Recycling and Application Possibilities: a Review. *Materials Science*. <https://matsc.ktu.lt/index.php/MatSc/article/view/26243>. Accessed 25 Sept 2021
 37. Genta M, Iwaya T, Sasaki M, Goto M (2007) Supercritical methanol for polyethylene terephthalate depolymerization: observation using simulator. *Waste Manag* 27:1167–1177. <https://doi.org/10.1016/j.wasman.2006.06.005>
 38. Goto M, Koyamoto H, Kodama A et al (2002) Depolymerization of polyethylene terephthalate in supercritical methanol. *J Phys Condens Matter* 14:11427–11430. <https://doi.org/10.1088/0953-8984/14/44/494>
 39. Sako T, Sugeta T, Otake K et al (1997) Depolymerization of polyethylene terephthalate to monomers with supercritical methanol. *J Chem Eng Japan* 30:342–346. <https://doi.org/10.1252/jcej.30.342>
 40. Yang Y, Lu Y, Xiang H et al (2002) Study on methanolytic depolymerization of PET with supercritical methanol for chemical recycling. *Polym Degrad Stab* 75:185–191. [https://doi.org/10.1016/S0141-3910\(01\)00217-8](https://doi.org/10.1016/S0141-3910(01)00217-8)
 41. Kurokawa H, Ohshima MA, Sugiyama K, Miura H (2003) Methanolysis of polyethylene terephthalate (PET) in the presence of aluminium triisopropoxide catalyst to form dimethyl terephthalate and ethylene glycol. *Polym Degrad Stab* 79:529–533. [https://doi.org/10.1016/S0141-3910\(02\)00370-1](https://doi.org/10.1016/S0141-3910(02)00370-1)
 42. Basumatary S, Nath B, Kalita P (2018) Application of agro-waste derived materials as heterogeneous base catalysts for biodiesel synthesis. *J Renew Sustain Energy* 10:043105. <https://doi.org/10.1063/1.5043328>
 43. Abdullah SHYS, Hanapi NHM, Azid A et al (2017) A review of biomass-derived heterogeneous catalyst for a sustainable biodiesel production. *Renew Sustain Energy Rev* 70:1040–1051. <https://doi.org/10.1016/J.RSER.2016.12.008>
 44. Lee D (2013) Preparation of a sulfonated carbonaceous material from lignosulfonate and its usefulness as an esterification catalyst. *Molecules* 18:8168–8180. <https://doi.org/10.3390/molecules18078168>
 45. Pathak G, Das D, Rajkumari K, Rokhum L (2018) Exploiting waste: towards a sustainable production of biodiesel using: *Musa acuminata* peel ash as a heterogeneous catalyst. *Green Chem* 20:2365–2373. <https://doi.org/10.1039/c8gc00071a>
 46. Nath B, Das B, Kalita P, Basumatary S (2019) Waste to value addition: utilization of waste *Brassica nigra* plant derived novel green heterogeneous base catalyst for effective synthesis of biodiesel. *J Clean Prod*. <https://doi.org/10.1016/j.jclepro.2019.118112>
 47. Rajkumari K, Das D, Pathak G, Rokhum L (2019) Waste-to-useful: a biowaste-derived heterogeneous catalyst for a green and sustainable Henry reaction. *New J Chem* 43:2134–2140. <https://doi.org/10.1039/c8nj05029e>
 48. Sarmah M, Dewan A, Mondal M et al (2016) Analysis of the water extract of waste papaya bark ash and its implications as an in situ base in the ligand-free recyclable Suzuki-Miyaura coupling reaction. *RSC Adv* 6:28981–28985. <https://doi.org/10.1039/c6ra00454g>
 49. Gohain M, Laskar K, Paul AK et al (2020) Carica papaya stem: a source of versatile heterogeneous catalyst for biodiesel production and C-C bond formation. *Renew Energy* 147:541–555. <https://doi.org/10.1016/j.renene.2019.09.016>
 50. Talukdar A, Deka DC (2020) Water hyacinth ash: an efficient green catalyst for the synthesis of β -amino carbonyl/nitrile compounds by aza-Michael reaction at room temperature. *SN Appl Sci*. <https://doi.org/10.1007/s42452-020-2281-7>
 51. Changmai B, Vanlalveni C, Ingle AP et al (2020) Widely used catalysts in biodiesel production: a review. *RSC Adv* 10:41625–41679. <https://doi.org/10.1039/D0RA07931F>
 52. Laldinpui Z, Lalmangaihuala S, Pachuau Z, Vanlaldinpuia K (2021) Depolymerization of poly(ethylene terephthalate) waste with biomass-waste derived recyclable heterogeneous catalyst. *Waste Manag* 126:1–10. <https://doi.org/10.1016/j.wasman.2021.02.056>
 53. Lalmangaihuala S, Laldinpui Z, Lalmuanpuia C, Vanlaldinpuia K (2021) Glycolysis of poly(ethylene terephthalate) using biomass-waste derived recyclable heterogeneous catalyst. *Polymers (Basel)* 13:1–13. <https://doi.org/10.3390/polym13010037>
 54. Laldinpui TZ, Lalmuanpuia C, Lalmangaihuala S et al (2021) Biomass waste-derived recyclable heterogeneous catalyst for aqueous aldol reaction and depolymerization of PET waste. *New J Chem*. <https://doi.org/10.1039/D1NJ03225A>
 55. Fei B, Gao Z, Wang J, Liu Z (2016) Biological, anatomical, and chemical characteristics of bamboo. *Second Xylem Biol Orig Funct Appl*. <https://doi.org/10.1016/B978-0-12-802185-9.00014-0>
 56. Fatimah I, Rubiyanto D, Taushiyah A et al (2019) Use of ZrO₂ supported on bamboo leaf ash as a heterogeneous catalyst in microwave-assisted biodiesel conversion. *Sustain Chem Pharm* 12:100129. <https://doi.org/10.1016/j.scp.2019.100129>
 57. Kow K, Yusoff R, Aziz ARA, Abdullah EC (2014) From bamboo leaf to aerogel: Preparation of water glass as a precursor. *J Non Cryst Solids* 386:76–84. <https://doi.org/10.1016/j.jnoncrysol.2013.11.041>
 58. Umoh AA, Odesola IA (2015) Characteristics of bamboo leaf ash blended cement paste and mortar. *Civ Eng Dimens* 17:22–28. <https://doi.org/10.9744/ced.17.1.22-28>
 59. Panowicz R, Konarzewski M, Durejko T et al (2021) Properties of polyethylene terephthalate (PET) after thermo-oxidative aging. *Materials* 14:3833. <https://doi.org/10.3390/MA14143833>
 60. Crystallization behavior of PET materials. <https://acikerisim.bartın.edu.tr/handle/11772/1592>. Accessed 25 Sept 2021
 61. Jenkins MJ, Harrison KL (2008) The effect of crystalline morphology on the degradation of polycaprolactone in a solution of phosphate buffer and lipase. *Polym Adv Technol* 19:1901–1906. <https://doi.org/10.1002/PAT.1227>
 62. Sing KSW, Williams RT (2004) Physisorption hysteresis loops and the characterization of nanoporous materials. *Adsorpt Sci Technol* 22:773–782. <https://doi.org/10.1260/0263617053499032>
 63. Chouhan APS, Sarma AK (2013) Biodiesel production from *Jatropha curcas* L. oil using *Lemma perpusilla* Torrey ash as heterogeneous catalyst. *Biomass Bioenergy* 55:386–389. <https://doi.org/10.1016/j.biombioe.2013.02.009>
 64. Changmai B, Rano R, Vanlalveni C, Rokhum L (2021) A novel *Citrus sinensis* peel ash coated magnetic nanoparticles as an easily recoverable solid catalyst for biodiesel production. *Fuel*. <https://doi.org/10.1016/j.fuel.2020.119447>
 65. Rajkumari K, Kalita J, Das D, Rokhum L (2017) Magnetic Fe₃O₄/silica sulfuric acid nanoparticles promoted regioselective protection/deprotection of alcohols with dihydropyran under solvent-free conditions. *RSC Adv* 7:56559–56565. <https://doi.org/10.1039/C7RA12458A>
 66. Teo SH, Islam A, Chan ES et al (2019) Efficient biodiesel production from *Jatropha curcas* using CaSO₄/Fe₂O₃-SiO₂ core-shell magnetic nanoparticles. *J Clean Prod* 208:816–826. <https://doi.org/10.1016/j.jclepro.2018.10.107>
 67. Pham DD, Cho J (2021) Low-energy catalytic methanolysis of poly(ethyleneterephthalate). *Green Chem* 23:511–525. <https://doi.org/10.1039/d0gc03536j>

68. Kim BK, Hwang GC, Bae SY et al (2001) Depolymerization of polyethyleneterephthalate in supercritical methanol. *J Appl Polym Sci* 81:2102–2108. <https://doi.org/10.1002/app.1645>
69. Nikje MMA, Nazari F (2006) Microwave-assisted depolymerization of poly(ethylene terephthalate) [PET] at atmospheric pressure. *Adv Polym Technol* 25:242–246. <https://doi.org/10.1002/adv.20080>
70. Basumatary B, Das B, Nath B, Basumatary S (2021) Synthesis and characterization of heterogeneous catalyst from sugarcane bagasse: Production of jatropha seed oil methyl esters. *Curr Res Green Sustain Chem* 4:100082. <https://doi.org/10.1016/J.CRGSC.2021.100082>
71. Mishra S, Goje AS (2003) Kinetic and thermodynamic study of methanolysis of poly(ethylene terephthalate) waste powder. *Polym Int* 52:337–342. <https://doi.org/10.1002/PI.1147>
72. Kint DPR, de Ilarduya AM, Bou JJ, Muñoz-Guerra S (2002) Poly(ethylene terephthalate) copolymers containing nitroterephthalic units. III. Methanolytic degradation. *J Polym Sci Part A* 40:2276–2285. <https://doi.org/10.1002/POLA.10305>

Publisher's Note Springer Nature remains neutral with regard to jurisdictional claims in published maps and institutional affiliations.